Available online at www.sciencedirect.com
SCIENCE DIRECT®
Journal of Nuclear Materials 329–333 (2004) 1107–1112
journal of nuclear materials
www.elsevier.com/locate/jnucmat

Specimen size effects on ductile–brittle transition temperature in Charpy impact testing

H. Kurishita [a,*], T. Yamamoto [b], M. Narui [a], H. Suwarno [a], T. Yoshitake [c], Y. Yano [c], M. Yamazaki [a], H. Matsui [a]

[a] International Research Center for Nuclear Material Science, Institute for Materials Research, Tohoku University, Oarai, Ibaraki-ken 311-1313, Japan
[b] Department of Chemical Engineering, UCSB, Santa Barbara, CA 93106-5080, USA
[c] Japan Nuclear Cycle Development Institute (JNC), Oarai, Ibaraki 311-1393, Japan

Abstract

One key issue for small specimen test techniques is to clarify specimen size effects on test results. In consideration of size effects on determining the ductile-to-brittle transition temperature (DBTT) in Charpy impact testing, a method to evaluate the plastic constraint loss for differently sized Charpy V-notch (CVN) specimens is proposed and applied to a ferritic–martensitic steel, 2WFK, developed by JNC. In the method, a constraint factor, α, that is an index of the plastic constraint is defined as $\alpha = \sigma^*/\sigma_y^*$. Here, σ^* is the critical cleavage fracture stress which is a material constant and σ_y^* is the uniaxial yield stress at the DBTT at the strain rate generated in the Charpy impact test. The procedures for evaluating each of σ^* and σ_y^* are described and a result of σ^* and σ_y^*, thus the value of α, is presented for different types of miniaturized and full-sized CVN specimens of 2WFK.

1. Introduction

Degradation of mechanical properties of structural materials exposed to irradiation environments is one of the critical issues that can determine their lifetime. In order to evaluate such degradation, small specimen test techniques in mechanical testing of irradiated materials is required because of a very limited irradiation volume in intense neutron sources such as IFMIF, as well as the minimization of a certain degree of inhomogeneity in flux and temperature distributions during irradiation.

An important measure of radiation embrittlement is a shift of the ductile-to-brittle transition temperature (DBTT). The DBTT shift due to irradiation is widely evaluated by using Charpy impact tests. It is, however, well known that the DBTT obtained in Charpy tests decreases with decreasing specimen size. Various empirical relationships between DBTT and specimen size and geometry have been proposed [1–9]. Such an empirical relationship is, however, questionable whenever the constitutive behavior of materials changes significantly, as is quite often the case for irradiated materials.

The effects of specimen size on DBTT in Charpy impact testing come from plastic constraint loss and statistical effects. This study focuses on the significance of plastic constraint to specimen size. Therefore, efforts to quantify specimen size effects due to constraint loss on DBTT are made for a ferritic–martensitic steel, 2WFK, developed by JNC.

2. Description of specimen size effects due to constraint loss on DBTT

In order to quantify specimen size effects due to constraint loss on DBTT in Charpy impact testing we propose

* Corresponding author. Tel.: +81-29 267 4157; fax: +81-29 267 4947.
E-mail address: kurishi@imr.tohoku.ac.jp (H. Kurishita).

0022-3115/$ - see front matter © 2004 Elsevier B.V. All rights reserved.
doi:10.1016/j.jnucmat.2004.04.307

a constraint factor, α, which is an index that expresses quantitatively the plastic constraint and is defined here as

$$\alpha = \sigma^*/\sigma_y, \tag{1}$$

where σ^* is the critical cleavage fracture stress, which is a material constant and can be determined from the finite element analysis (FEA) based on the critical stress – stressed area, A^*, model [10–12]. At the critical opening displacement of a notch for cleavage initiation, the averaged area stressed higher than σ^* within the planes perpendicular to notch front line reaches A^*. The σ_y^* is the uniaxial yield stress at the DBTT of the material in question at the strain rate generated in the Charpy impact test. The DBTT is defined here as the temperature where cleavage crack starts after certain amount of plastic deformation. The definition suggests that there is a common level of deformation for cleavage initiation at the DBTT regardless of material. For a particular specimen geometry (particular ratios of thickness, B, notch depth, a, and notch root radius, ρ, to width, W), the value of A^* normalized by the square of specimen ligament, b, can be expressed by a common function of the σ^* normalized by σ_y^* which actually is α as,

$$A^*/b^2 = f(\alpha). \tag{2}$$

The α_{full} for the full size specimen of a material can be determined from subsize specimen data $\alpha_{sub}(=\sigma^*/\sigma_y^*(T_{sub}))$ and ligament sizes, b_{sub} and b_{full}, using this function $f(\alpha)$ and the T-dependence of $\sigma_y^*(T)$ of the material.

The practical procedure for evaluating α is as follows.

(1) Evaluate the critical stress, σ^*, and critical area, A^*, for the initiation of cleavage fracture in the Charpy impact test by FEA.
(2) Evaluate the uniaxial yield strength, σ_y, at the same strain rate as that is generated in the Charpy impact test as a function of test temperature for unnotched, smooth bend specimens.
(3) Determine the DBTT as a function of specimen size.
(4) Evaluate σ_y at the DBTT, σ_y^*, as a function of specimen size.
(5) Evaluate $\alpha = \sigma^*/\sigma_y$ as a function of specimen size and examine the dependence of α on specimen size.
(6) Conduct the same evaluation as the above on several materials and compare the dependency among the materials.

As a result, if α is independent of material properties, the DBTT of the full size specimen can be determined from only the data of miniaturized specimens. If α shows a dependency, it can be evaluated by a quantitative relationship between α and material properties.

3. Experimental

The above method requires mechanical tests, such as Charpy impact tests, tensile tests, three-point bend tests, and three-dimensional (3D) simulations of specimen deformation.

Three types of specimens were machined from a ferritic-martensitic steel, 2WFK, in the unaged condition. This was developed by JNC and has the chemical composition shown in Table 1. The specimens were (1) the full size Charpy V-notch (CVN) and miniaturized Charpy V-notch (MCVN) specimens with different sizes and notch geometries, (2) three-point bend specimens, and (3) tensile specimens. The latter two were fabricated from the broken halves of the CVN specimens and have dimensions of 1.5 mm in width and 0.5 mm in thickness. For the size and notch dimensions of the MCVN specimens see Table 2.

Charpy impact tests were conducted at temperatures from 137 to 300 K at a displacement rate of approximately 5 m s^{-1} by using a specially designed instrumented machine [4]. Three-point bend tests were carried out at temperatures from 77 to 290 K at displacement rates from 0.0013 to 13 mm s^{-1} with a span of 7.07 mm. Tensile tests were performed at temperatures from 163 to 293 K at displacement rates from 0.005 to 50 mm s^{-1}, which correspond to initial strain rates of 1×10^{-3} to 10 s^{-1}. For both the three-point bend and tensile tests, a servo-hydraulic fatigue testing machine (Shimadzu Servopulser of 50-kN capacity equipped with a 5-kN shear-type load cell) was used. For high-speed tests with displacement rates above 5 mm s^{-1} a quartz load washer (capacity 750 kN), which utilizes the piezoeffect, was used to measure the applied load instead of a load cell.

Three dimensional (3D) simulations of the specimen deformation were analyzed using the finite element code, ABAQUS. Using symmetry, one fourth of the specimen within the span was modeled. The impact tests were treated as static processes with a constitutive equation corresponding to high strain rate deformation.

4. Results and discussion

In order to obtain the constitutive equation used in the FEA at arbitrary temperatures and strain rates, true

Table 1
Chemical compositions of ferritic–martensitic steel, 2WFK in the unaged condition (wt%)

C	Si	Mn	Cr	Ni	Mo	V	W	Fe
0.12	0.05	0.60	11.0	0.40	0.50	0.20	2.0	Bal.

Table 2
Values of DBTT, σ_y^* and α evaluated for full size and miniaturized CVN specimens with different V-notch sizes of unaged 2WFK

Specimen size	V-notch size (ρ/mm–a/mm–θ/degree)	DBTT (K)	σ_y^* (MPa)	$\alpha = \sigma^*/\sigma_y^*$
Full Size	0.25–2.0–45	287	915	2.62
3.3×3.3 mm	0.08–0.50–30	224	998	2.40
3.3×3.3 mm	0.02–0.50–30	236	980	2.45
3.3×3.3 mm	0.02–0.65–30	260	948	2.53
2.0×2.0 mm	0.08–0.40–30	227	994	2.42
2.0×2.0 mm	0.02–0.40–30	235	982	2.44
2.0×2.0 mm	0.02–0.60–30	240	975	2.46
1.5×1.5 mm	0.08–0.30–30	178	1079	2.23
1.5×1.5 mm	0.02–0.30–30	198	1041	2.31
1.5×1.5 mm	0.02–0.45–30	212	1017	2.36
1.0×1.0 mm	0.05–0.20–30	150	1139	2.11
1.0×1.0 mm	0.02–0.30–30	181	1073	2.24

stress–strain curves for the unaged 2WFK were measured at various temperatures and strain rates. As a result, it was found that stress–strain curves at arbitrary temperatures and strain rates can be represented by

$$\sigma = \sigma_{0.001} + \sigma_{\text{sat}}[1 - \exp\{-k(\varepsilon_p - 0.001)\}]^{1/2}. \quad (3)$$

Here, $\sigma_{0.001}$ is the true stress at 0.1% plastic strain and defined here as the yield stress, σ_{sat} is the saturated hardening and k is a rate constant [13]. The curve calculated by the above relation is shown in Fig. 1 together with that calculated by the power law relation. Comparison of the two curves indicates that the above relation slightly improves the reproducibility of the experimental curve.

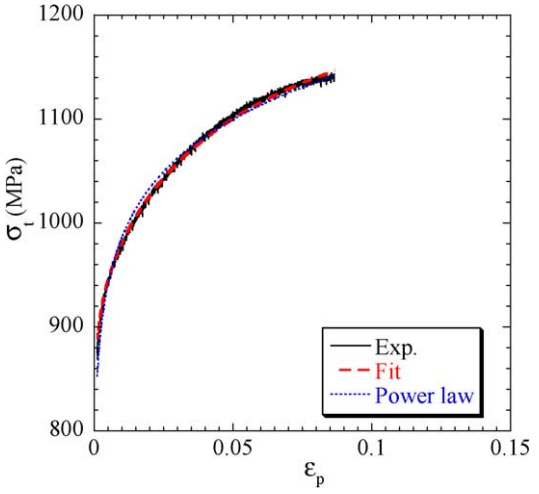

Fig. 1. Comparison between the true stress–true strain curves calculated by Eq. (3) (fit) and the power low relation and by experiment for unaged 2WFK specimen tested at 223 K and 1×10^{-3} s^{-1}.

The three parameters of $\sigma_{0.001}, \sigma_{\text{sat}}$ and k can be expressed by the following equations:

$$\sigma_{0.001} = \sigma_{\text{th}}(T^*) + \sigma_{\text{ath}}(T), \quad (4)$$

$$\sigma_{\text{sat}} = -1.05T + 600, \quad (5)$$

$$k = 2.380 \times 10^{-4} T^{1.998}, \quad (6)$$

where $\sigma_{\text{th}}(T^*)$ is the effective stress component that is temperature and strain rate dependent and $\sigma_{\text{ath}}(T)$ is the internal stress component that is slightly dependent on temperature due to the temperature dependence of the shear modulus. $\sigma_{\text{th}}(T^*), \sigma_{\text{ath}}(T)$ and T^* are given by

$$\sigma_{\text{th}}(T^*) = 1253.6[1 - (T^*/14990)^{1/2}]^2, \quad (7)$$

$$\sigma_{\text{ath}}(T) = 891(1 - 0.00028T), \quad (8)$$

$$T^* = T\ln(7.78\,\text{e}^{15}/\dot{\varepsilon}) \quad (9)$$

Fig. 2 shows comparison of load vs. displacement curves recorded by Charpy impact tests at 193 K for third-sized specimens with simulated curves based on the above constitutive equation. The experimental curve is well represented by the simulated curve.

In order to determine σ^*–A^* values, the stress fields ahead of the notch at cleavage crack initiation were calculated by FEA with the above constitutive equation and the σ–A curves were obtained as shown in Fig. 3. The change of A against notch opening displacement, Δ, in the region of lower shelf energy (LSE) for the full size specimen was large and caused large scattering compared to the absorbed energy–temperature curve. However, for each sized specimens, the scattering occurs without appreciable change in shape of the curves, i.e., the three curves for each sized specimens shift in almost parallel. This may reflect inhomogeneous distributions

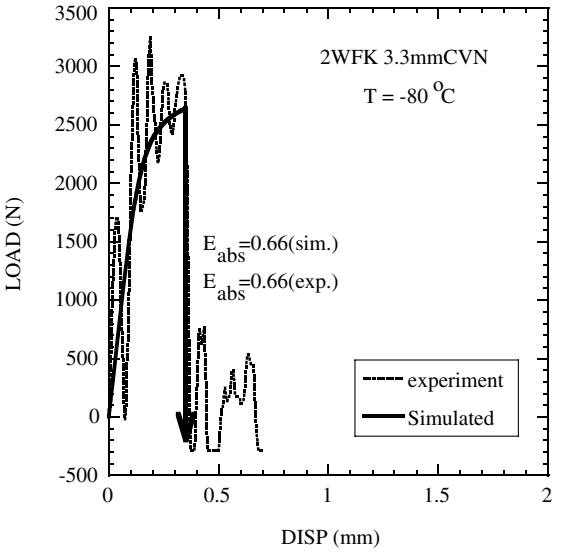

Fig. 2. Comparison of load vs. displacement curves recorded by Charpy impact tests at 193 K for third-sized specimens of unaged 2WFK with simulated curves based on the constitutive equation.

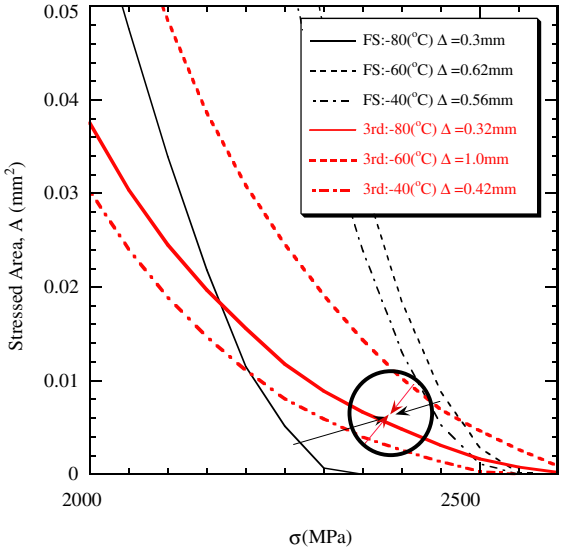

Fig. 3. Plot of stressed area, A, against stress, σ, ahead of the notch with different opening displacements, Δ, simulated by 3D FEA with the constitutive equation for full sized and third sized specimens of unaged 2WFK.

of crack initiation sites. Therefore, we averaged the three curves for the each sized specimens. The averaged curves obtained for the CVN and third-sized specimens intersected at $\sigma = 2400$ MPa and $A = 0.0065$ mm^2, which may correspond to the critical cleavage stress σ^* and area A^* that are independent of specimen size, i.e., $\sigma^* = 2400$ MPa, $A^* = 0.0065$ mm^2.

Next, to evaluate the uniaxial yield strength, σ_y, at the same strain rate as that generated in the Charpy impact test as a function of test temperature for unnotched, smooth bend specimens, correlation between each of the yield stresses obtained by three-point bend tests and tensile tests is necessary to be expressed as a function of strain rate. Therefore, the FEM analysis with the above constitutive equation with the ABAQUS code was made to simulate the three-point load–deflection curves of the unaged 2WFK. The following correlation equations were found between the yield stresses by three-point bend tests, σ_y^b, and that by tensile tests, σ_y, and the strain hardening exponents by three-point bend tests, n^b, and that by tensile tests, n.

$$\sigma_y^b = \sigma_y(0.82 + 1.16n^t - 0.767n^{t2}). \tag{10}$$

$$n^b = 0.0311 + 0.978n. \tag{11}$$

The details will be described elsewhere [14]. These equations were applied to obtain the uniaxial yield strength, σ_y, and the strain hardening exponents, n, for the unaged 2WFK from the experimental three-point bend test results for the unnotched, smooth specimens. Thus the obtained values of σ_y and n and their experimental values are plotted against strain rate. No significant differences were recognized between both the data, although difference had a tendency to increase with increasing strain rate. Therefore, the simulated values of σ_y were extrapolated to the high strain rate corresponding to that in the Charpy impact test, assuming here a linear approximation. The strain rate at the front of the notch should be used and is estimated to be about 10^3–10^4 s^{-1}, and 10^3 s^{-1} was used here. In this way, the uniaxial yield strength, σ_y, at 10^3 s^{-1} was obtained as a function of test temperature.

Thirdly, the DBTT, which is here defined as the temperature where the absorbed energy is equal to 41 J for the full size specimen, is shown in Table 2 for CVN and MCVN specimens with different V-notch sizes (ρ–a–θ) of the unaged 2WFK, where ρ is the notch root radius, a is the notch depth and θ is the notch angle. From the above results, σ_y at the DBTT, which is defined here as σ_y^*, can be evaluated as a function of specimen size and V-notch size.

Finally, substituting the evaluated values of σ^* and σ_y^* into Eq. (1) gives α values, which are shown in Table 2 and Fig. 4 as a function of A^*/b^2. The uncertainty of α may be approximately ±4%, considering those of σ^* (±50 MPa, ±2%) and $\sigma_{0.001}$ (±20 MPa, ±2%). Theoretical α–A^*/b^2 curve has not been obtained due to the lack of sufficient information on a proper deformation level at DBTT. However, it is considered that the σ–A profile for the third size specimen tested at 213 K (−60 °C)

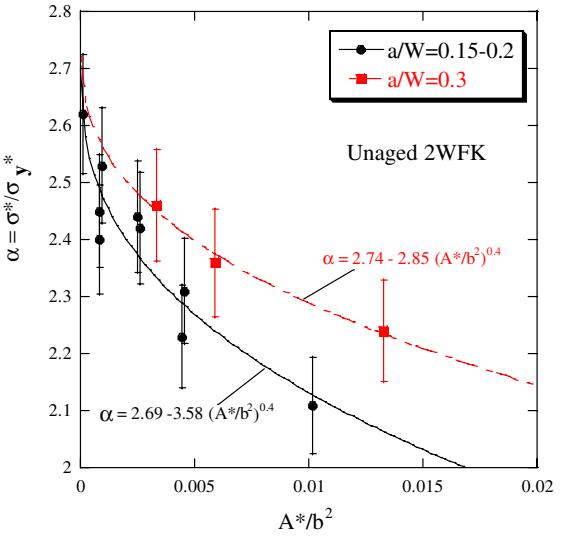

Fig. 4. Plot of α against specimen size parameter A^*/b^2 for CVN and MCVN specimens with different geometries of unaged 2WFK.

showing the absorbed energy of 40%USE, which is relatively close to 30%USE corresponding to the above value of 41 J for the full size specimen may give a useful suggestion on the curve. The α–A^*/b^2 curve obtained from the σ–A profile revealed that it is formulated as $\alpha = \alpha_0 - c(A^*/b^2)^{0.4}$ in the range of the α from 1.9 to 2.6. Thus the formula was applied to obtain a semi-empirical relation of the α–A^*/b^2 curves. The values of α_0 and c were determined as 2.69 and 3.58 for the data with a/W from 0.15 to 0.2, while 2.74 and 2.85 for the data with a/W of 0.3. Effects of notch geometry on the curves were not significant. The two different curves clearly show the contribution of deeper notch to higher constraint.

It was shown that α which is necessary to describe the specimen size effects can be evaluated as a function of specimen size. The next problems are to increase the measurement accuracy of α, evaluate specimen size dependence of α for a ferritic steel different from the unaged 2WK and establish a quantitative expression of dependence on materials property if the size dependence exhibits a tendency of variation among materials.

5. Conclusions

(1) A method to quantify specimen size effects on DBTT in Charpy impact testing from the viewpoint of plastic constraint loss was proposed and applied to a ferritic–martensitic steel, 2WFK, developed by JNC. In the method a constraint factor, α, that is an index of the plastic constraint is defined as $\alpha = \sigma^*/\sigma_y^*$. Here, σ^* is the critical cleavage fracture stress and a material constant and σ_y^* is the uniaxial yield stress at the DBTT at the strain rate generated in the Charpy impact test.

(2) A constitutive equation for describing stress-strain curves of the unaged 2WFK at arbitrary temperatures and strain rates was obtained. Three dimensional FEA simulations of the impact test with this constitutive equation and a cleavage fracture model that is based on a critical stress–critical area plot led to evaluation of the critical cleavage stress σ^* and area A^*.

(3) A correlation equation to obtain the uniaxial yield strength, σ_y, and the strain hardening exponents, n, for the unaged 2WFK from the experimental three-point bend test results was introduced. Extrapolating σ_y to 10^3 s^{-1} led to the evaluation of σ_y at the strain rate close to that generated in the Charpy impact test as a function of test temperature.

(4) The DBTT at 41 J for the full size specimens was evaluated for differently sized Charpy specimens for the unaged 2WFK, and the value of σ_y^*, that is σ_y at the DBTT, was evaluated as a function of specimen size and V-notch size.

(5) The values of α were evaluated for the full size and miniaturized CVD specimens. They showed a reasonable relationship with specimen size parameter A^*/b^2 for differently sized specimens of unaged 2WFK.

Acknowledgements

The authors would like to express their gratitude to Dr S. Matsuo for his review.

References

[1] G.E. Lucus, G.R. Odette, J.W. Sheckherd, P. McConnell, J. Perrin, ASTM STP 888 (1986) 305.
[2] B.S. Louden, A.S. Kumar, F.A. Garner, M.L. Hamilton, W.L. Hu, J. Nucl. Mater. 155 (1988) 662.
[3] D.J. Alexander, R.L. Klueh, ASTM STP 1072 (1990) 179.
[4] H. Kayano, H. Kurishita, M. Narui, M. Yamazaki, Ann. Chem. Fr. 16 (1991) 309.
[5] H. Kayano, H. Kurishita, A. Kimura, M. Narui, M. Yamazaki, Y. Suzuki, J. Nucl. Mater. 179 (1991) 425.
[6] H. Kurishita, H. Kayano, M. Narui, M. Yamazaki, Y. Kano, I. Shibahara, Mate. Trans. JIM 34 (1993) 1042.
[7] M.A. Sokolov, R.K. Nanstad, ASTM STP 1270 (1996) 384.
[8] G.E. Lucus, G.R. Odette, K. Edsinger, B.D. Wirth, J.W. Sheckherd, ASTM STP 1270 (1996) 790.
[9] K. Doi, N. Soneda, T. Onchi, H. Matsui, ASTM STP 1428 (2002) 137.
[10] T. Yamamoto, G.R. Odette, G.E. Lucas, H. Matsui, J. Nucl. Mater. 283–287 (2000) 992.

[11] T. Yamamoto, K. Yabuki, H. Matsui, G.R. Odette, G.E. Lucas, ASTM STP 1418 (2001) 93.
[12] G.R. Odette, J. Nucl. Mater. 212–215 (1994) 45.
[13] P. Spatig, G.R. Odette, G.E. Lucas, M. Victoria, J. Nucl. Mater. 307–311 (2002) 536.
[14] T. Yamamoto, H. Kurishita, H. Swarno, in preparation.